GEOTHERMAL TEMPERATURE ESTIMATION BASED ON RESISTIVITY DATA USING ARTIFICIAL NEURAL NETWORK: APPLICATION TO THE KAKKONDA GEOTHERMAL FIELD, JAPAN

Kazuya Ishitsuka[1], Toru Mogi[1], Kotaro Sugano[2], Toshihiro Uchida[3] and Tatsuya Kajiwara[4]

[1]Division of Sustainable Resources Engineering, Hokkaido University
Kita 13 Nishi 8, Kita-ku, Sapporo, Hokkaido, 060-8628, Japan

[2] Hokkaido Electric Power Co., Inc.
1-2 Oodori Higashi, Chuou-ku, Sapporo, Hokkaido, 060-8677, Japan

[3] Geological Survey of Japan, National Institute of Advanced Industrial Science and Technology
1-1-1 Higashi, Tsukuba, Ibaraki 305-8567, Japan

[4] Geothermal Engineering Co., Ltd.
356-6 Ooshimizu, Oogama, Takizawa, Iwate, 020-0758, Japan

ishitsuka@eng.hokudai.ac.jp

Keywords: *Temperature estimation, Artificial Neural Network, the Kakkonda Geothermal Field, Resistivity*

ABSTRACT

Temperature distribution at a geothermal development provides a vital information for geothermal development. Spichak et al. (2007) has proposed to use artificial neural network estimation to estimate temperature distribution based on resistivity data by Magnetotelluric observation. In this study, we examined the characteristics of the neural network approach at the Kakkonda Geothermal Field in Japan. Temperature data measured at wells were used, including the deepest well of WD1 with the depth of about 3700 m penetrating granite basement rock. Through the application, we showed the importance of the 2D location of teaching data. Specifically, the error increases when teaching data were far from target area. By optimizing the structure of a neural network, we demonstrated that the error of the estimated WD1 temperature was 16 %, and the estimated temperature pattern almost agree with the observed temperature. In addition, we proposed another temperature estimation approach based on neural kriging. Since the neural kriging accounts for variogram of temperature data, underlying statistical structure reflects estimated temperature. As a result of validation, we showed that the estimated temperature successfully reduced the error of data variogram. This result demonstrates the effectiveness of the neural network and neural kriging approach with temperature for estimating temperature at deeper parts.

1. INTRODUCTION

Subsurface temperature estimation at a geothermal area is important to understand a geothermal system of the area. Direct measurement of subsurface temperature is generally done at the location of borehole, and additional information or assumptions is required to estimate subsurface temperature structure at areas without borehole location. Recently, Spichak et al. (2007) and Spichak and Zakharova (2009) have proposed to use resistivity data to estimate temperature distribution by means of artificial neural network. It is well known that resistivity is sensitive to temperature, clay content and rock type. Especially, we focus on the influence of temperature to resistivity. The underlying mechanism is that pore fluid viscosity, which is a major conductive medium, decreases with increasing temperature [Yokoyama et al., 1983].

This method firstly constructs a neural network model that relates between resistivity and temperature at the location of borehole wells. Then, the constructed neural network is applied to estimate temperature based on resistivity distribution at the location without borehole data. The method utilizes resistivity data as an indirect geothermometer, and enables to represent complex resisitivity-temperature relationship that depends on each target site.

Another standard method to estimate temperature distribution is kriging interpolation [e.g., Masaji, 2005]. The kriging interpolation method uses the statistical structure of a priori known temperature data (e.g., temperature measure at borehole wells) via variogram. Koike et al. (2001) has proposed neural kriging method that combines kriging and neural network for interpolation of observed data. This method constructs neural network application by satisfying variogram.

In this study, we examined the characteristics of the proposed neural network approach through the application to the Kakkonda Geothermal Field located at northern Japan. Moreover, we proposed a method to estimate subsurface temperature structure based on neural kriging. The neural network approach constructs a network based on temperature-resistivity relationship at well locations. On the other hand, the neural kriging approach constructs a network accounting for variogram of the temperature data in addition to temperature-resistivity relationship.

The Kakkonda Geothermal Field is one of the largest and most active liquid-dominated geothermal systems in Japan. The No. 1 unit has generated 50 MW of peak power since 1978, and the No. 2 unit has generated 30 MW of peak power since 1996. The deepest borehole drill is 3729 m depth and the maximum temperature is about 500 ℃. The deepest well penetrates the Kakkonda granite below about 2860 m, where it is interpreted as heat sources of the geothermal field. Through the application to the geothermal field, we aim at estimating temperature structure deeper than borehole locations in addition to surrounding areas.

2. SUBSURFACE TEMPERATURE ESTIMATION

2.1 Neural network approach based on resistivity data

Neural network is a computer algorithm that is an analog of neurons in human brain. The algorithm has been widely used to estimate geophysical parameters [Calderon-Macias et al., 2000; van der Baan and Jutten, 2000]. The neural network consists of a number of units called perceptrons and nodes between the perceptrons. One perceptron reads the weighted sum of inputs (x_i) and calculates an output (y) though a certain functional relationship (Figure 1a; Eq. 1). Generally, two kinds of coefficients are used for a perceptron: one is weights of each input (w_i), another is a threshold or bias that is subtracted from the weighted sum of inputs (h). The number of weights corresponds to the number of nodes, and the number of thresholds correspond to the number of perceptrons.

$$y = f\left(\sum_i w_i x_i - h \right) \qquad (1)$$

Generally, artificial neural network consists of a number of perceptrons arranged in multi-layer. A multi-layer neural network has hidden layers between an input and output layer (Figure 1b). The unknown coefficients are estimated in learning processes. The learning process uses teaching data to estimate optimal coefficients by minimizing the square difference between outputs and the teaching data (Eq. 2). The learning process continues until the square difference becomes at a sufficiently small value.

$$F_{NN} = \sum_i \left(y_{obs,i} - y_{est,i} \right)^2 \qquad (2)$$

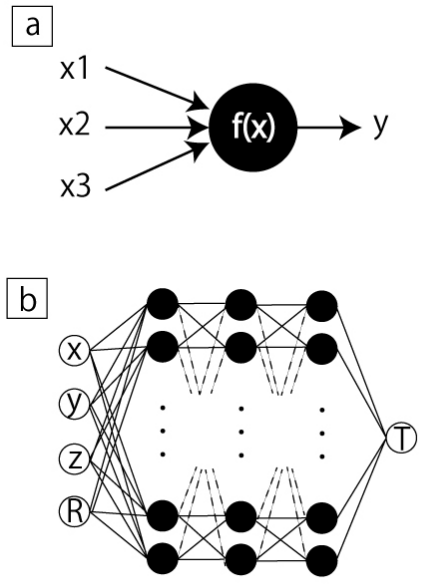

Figure 1: (a) The basic concept of a perceptron in neural network. (b) The basic concept of multi-layer neural network used in this study. The symbols x, y, z indicate 3D locations, and R and T indicate resistivity and temperature, respectively.

One of the common algorithms of the optimization processes is back propagation method [Rumelhart and McClelland, 1988]. This method is based on steepest descent algorithm, and updates coefficients iteratively (Eq. 3 and 4). With these structures and strategies, neural network enables to approximate any kind of relationships between inputs and outputs.

$$w_{k+1} = w_k + \alpha_w \frac{\partial E_k}{\partial w} \qquad (3)$$

$$h_{k+1} = h_k + \alpha_h \frac{\partial E_k}{\partial h} \qquad (4)$$

In this study, we used temperature data measured at well locations as a teaching data of the outputs. Input data are 3D locations and resistivity. Parameters of a neural network are firstly estimated using the back propagation algorithm. Then, temperature at locations without teaching data are estimated by the optimized network.

The accuracy of the neural network estimation was evaluated by the difference between validation data and estimation data. Validation data were selected apart from teaching data, and the accuracy was evaluated by the difference using a neural network constructed by teaching data. As the index of accuracy, we used the relative error according to Spichak and Zakharova (2009) (Eq. 5).

$$Er = \sqrt{\frac{\sum_i \left(T_{obs,i} - T_{est,i} \right)^2}{\sum_i T_{obs,i}^2}} \qquad (5)$$

Where T_{obs} and T_{est} indicate observed and estimated temperature, respectively.

2.2 Neural kriging approach based on resistivity data

It is well known that kriging is an effective interpolation method, which is based on statistical structure characterized by variogram. The kriging approach assumes the principle that the surrounding data are more related to each other than those far apart. Previous studies successfully applied the kriging approach to underground thermal structure [e.g., Tian et al., 2015]. Since variogram represents spatial structure of data statistically, kriging interpolation can reveal parameter distribution based on location pattern.

By considering spatial structure pattern in neural network interpolation, neural kriging has been proposed [Koike et al., 2001]. Neural kriging incorporates the error of variogram as well as square difference into a learning criterion (Eq. 6).

$$F_{NK} = \frac{1}{n_1} \sum_i^{n_1} \left(\frac{y_{obs,i} - y_{est,i}}{\overline{y_{est}}} \right)^2 + \frac{1}{n_2} \sum_i^{n_2} \left(\frac{\gamma(h_i) - \gamma_e(h_i)}{\overline{\gamma}} \right)^2 \qquad (6)$$

where $\overline{y}_{est}$ is the average of teaching data, and h_i is the distance of the i th data. $\gamma(h_i)$ and $\gamma_e(h_i)$ are variogram of temperature teaching data and variogram of temperature data estimated by a neural network, respectively.

The back propagation algorithm is based on steepest descent in the nonlinear least squares method, which tends to fall local minimum. For the ptimization of neural kriging, we used genetic algorithm [Sen and Stoffa, 1995], which has strategies to avoid local minimum.

2.3 Data at the Kakkonda Geothermal Field

The Kakkonda Geothermal Field is one of the biggest geothermal field in northern Japan (Figure 2a). The geology of the Kakkonda Geothermal Field consists of pre- tertiary to Quaternary sedimentary and volcanic rocks intruded by Tertiary tonalite, the Matsuzawa dacite and the Torigoenotaki dacite (Figure 2b). The Quaternary Kakkonda granite is beneath the Tertiary and Pre-tertiary formation, and the granite is thought to be a heat source of the geothermal system (Figure 2b).

We used data from 7 wells at the Kakkonda Geothermal Field (Table 1; Figure 2b). The maximum depths of the wells are ranged from 892 to 3700 m. The temperature data at three wells were measured before the power plant operation. The other temperature data were measured after the operation. The well WD1 drilled in 1994 recorded a depth of 3729 m, which is the deepest well among the temperature data used in this study. The WD-1 penetrate the Kakkonda granite below about 2860 m. The temperature gradient sharply increased below about 3200 m [Ikeuchi et al., 1998]. The temperature at 3700 m is about 500 ℃. The temperature profile implies that the Kakkonda granite acts as the thermal conductive zone, whereas the shallower region is the thermal convective zone.

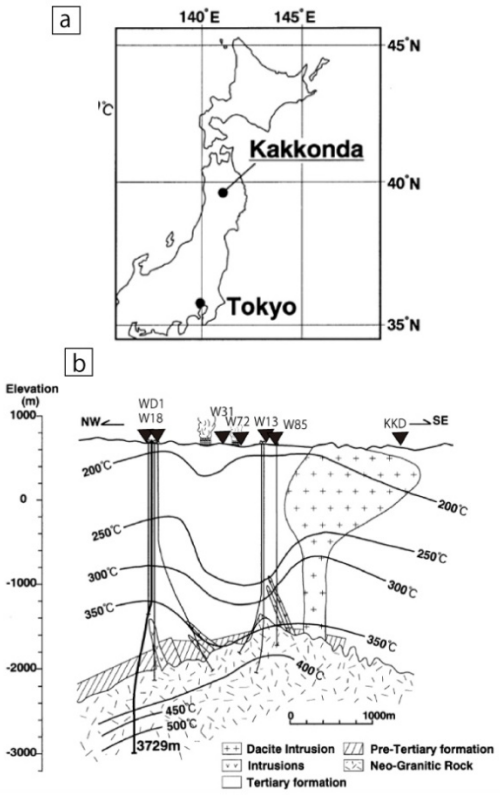

Figure 2: (a) The location of the Kakkonda Geothermal Field, (b) The geology around the Kakkonda Geothermal Field and the well locations (based on Kasai et al. (1998))

In well 18, there is an abrupt increase in temperature around the depth of 1400-1500 m. This depth is interpreted as the boundary between the shallow and the deep reservoir. The shallow reservoir lies above about 1500 m depth with permeable zone. On the other hand, it is known that the deep reservoir below 1500 m is less permeable, though the density of fracture is almost same as the shallow one [Kato et al., 1998]. The two reservoirs are hydraulically connected [Hanano, 1995].

We used resistivity data from MT analysis acquired along the valley aligned in the NW-SE (Figure 3) [Uchida et al., 2003]. The resistivity cross section reveals three characteristics. First is the low resistivity zone (0-10 Ohm m) below 200-1000 m, which corresponds to the altered clay constructing caprock layers (Figure 3). Second is moderate resistivity zone (10-100 Ohm m) in the depth of 1000–3000 m, which correspond to reservoir zones (Figure 3). In fact, lithology profiles in logs shows two major reservoir zones with the area: one is between 1000-2000 m area with fractured zones, the other is between about 2000-2500 m with less permeable zone. The final one is low resistivity zone (0-10 Ohm m) deeper than 3000 m (Figure 3).

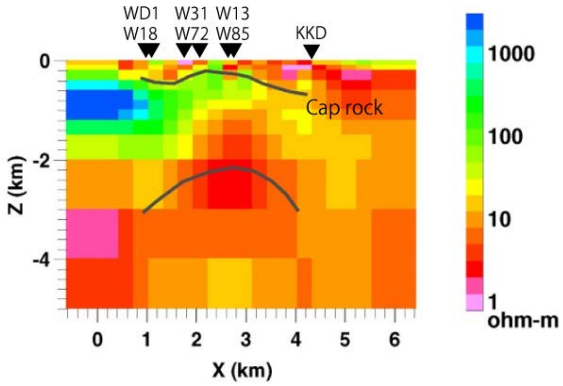

Figure 3: Resistivity cross-section around the Kakkonda Geothermal Field obtained from 3D inversion of magnetelluric data (based on Uchida et al. (2003)).

Table 1: Basic information of temperature data used in this study.

	W13	W18	W31	W72	W85	KKD	WD1
Maximum Depth [m]	2440	1890	1000	892	950	1150	3700
Maximum Temperature [deg]	355	345	229	234	227	259	510
The number of temperature data	35	17	13	18	19	19	45

3. RESULTS OF NEURAL NETWORK APPROACH

3.1 Sensitivity test

It is known that the selection of training data is important. We first evaluated the accuracy of neural network estimation depending on (i) the ratio of teaching data and (ii) wells used as a teaching data. In this evaluation, we set the number of layers is 3 and the number of perceptrons is 20 per a layer.

To examine the error simply depending on the number of teaching data, we randomly divided temperature data and resistivity data into teaching and evaluation data groups at a certain ratio. The ratios of the teaching data we examined in this study were 10, 30, 50, 70 and 90 % of all of data, and the rest of data were used as an evaluation data group, which were used to calculate the relative error.

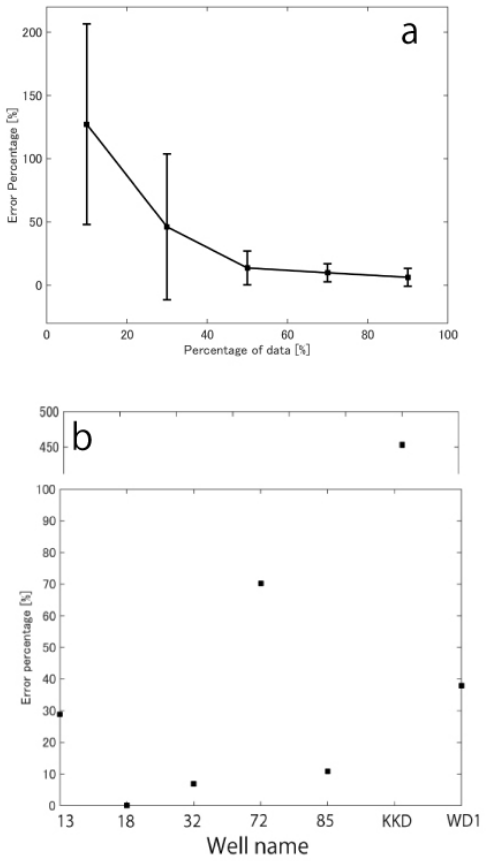

Figure 4: Errors of the neural network estimation. (a) the result depending on the number of data, (b) the result depending on the well number.

The relative error decreased with increasing the ratio of teaching data (Figure 4a). The mean of the error was 131 % when 10 % of total data were used as a training data, while the error was 6 % when the ratio of teaching data was 90 % (Figure 4a). Especially, the error did not significantly decrease when the ratio of teaching data was over 50 %. This indicates that almost half part of teaching data is enough to explain the relationship between the inputs (locations and resistivities) and the outputs (temperatures) in terms of statistical viewpoint.

We then examined the error depending on wells. One well is set to be validation data, and other wells are used as teaching data. The relative error is calculated in each well. In Figure 4b, the error was plotted, when each well was used as validation data. The error was mostly less than 30 %, which indicates the temperature variation in most of wells can be estimated by other well accurately. On the other hand, the error of well KKD was larger than other wells (> 400 %). This is likely because the location of KKD is far from other wells. Since the location is one of input parameters, the estimation at far from teaching data can cause inaccurate output. This result implies that the locations of teaching data and the target site is important to avoid significant error.

3.2 The estimation of temperature at well WD1

Well WD1 has the depth of 3729 m. This well penetrates granite bedrock under about 2860 m, which is known as thermal source of the geothermal field. Therefore, by evaluating the error of the WD1 well, we examined the applicability of this method to a deeper location.

It is known that outputs of a neural network also depend on the number of layers and perceptrons. Thus, we examined the error of WD1 temperature depending on the number of layers and perceptrons. We tested the number of layers is 1, 2, 3, 4, 5 (5 candidates), and the number of perceptrons per a layer is 5, 10, 15, 20 (4 candidates). We set the number of perceptrons is identical to all of layers. Considering the dependence on an initial value of weights and biases, we repeated the back propagation optimization by 50 times with different initial values. Then, we evaluated the accuracy in terms of minimum value of error ratio and the standard deviation of error ratio (Figure 5).

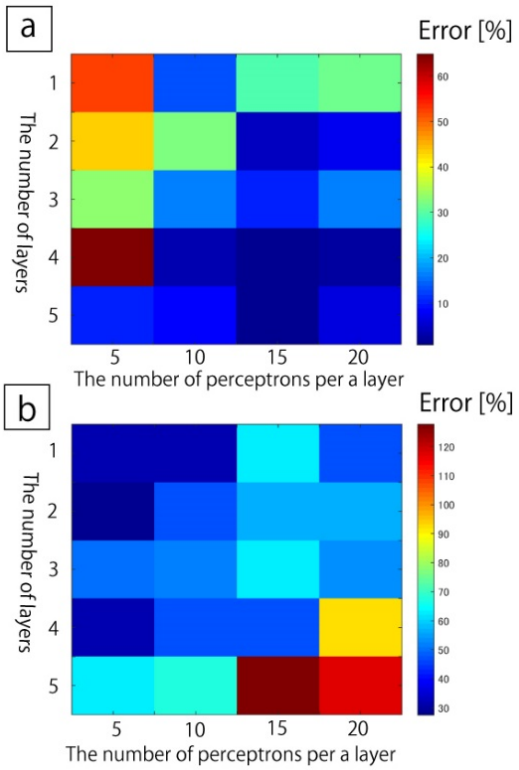

Figure 5: (a) the minimum value of the estimated error in each number of layers and perceptrons, (b) the standard deviation of the estimated error.

According to Figure 5a, the minimum value of the error basically decreased with increasing the number of layers and perceptrons. Especially, the number of layers is 3 and more, the error became less than 35 %, and perceptrons per a layer exceeds 20, the error was less than 20 %. On the other hand, the standard deviation basically increased with increasing the number of layers and perceptrons. Especially, when the number of perceptrons is over 20 and the number of layer is 3 and more, the standard deviation was less than 100 %. This indicates that the back propagation algorithm

converged to a local minimum, when the complexity of network increased. Then, we concluded that an optimal structure of neural network has the numbers of layers and the number of perceptrons per a layer of (4 and 15), because both the error and the standard deviation were small. In this case, we found the error of validation data was 16 % (Figure 6 and 7). Alternatively, the numbers of layer and the number of perceptrons per a layer of (3 and 20) and (5 and 10) were also an optimal structure. This result demonstrates that the effectiveness of the neural network approach to estimate deeper part of temperature.

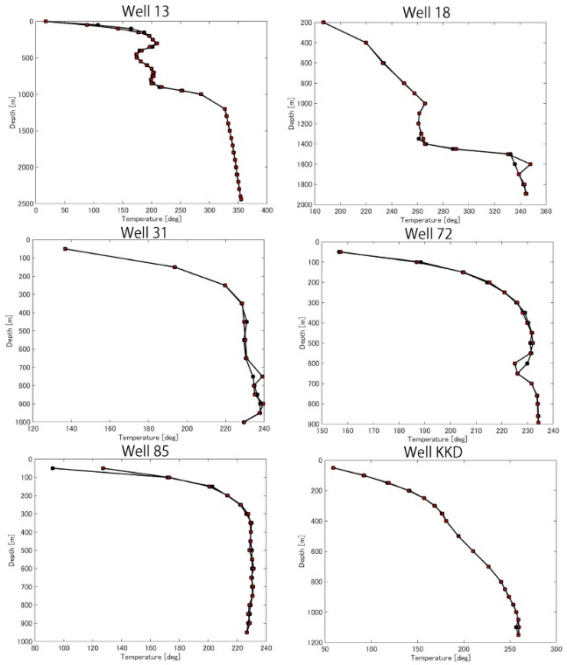

Figure 6: The comparison of teaching data. Black squares are observed temperature structures, and red squares are the estimated temperature structure by neural network with 4 layers and 15 perceptrons per a layer.

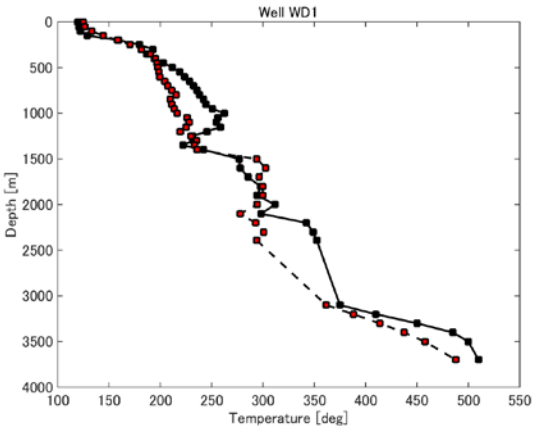

Figure 7: The comparison of validation data. Black squares are observed temperature structures, and red squares are the estimated temperature structure by neural network with 4 layers and 15 perceptrons per a layer.

We also note the characterisitcs of error depending on the number of layers and perceptrons. When a neural network had smaller number of layers and perceptrons (e.g., the number of layer and perceptrons were 1 and 5, respectively), the estimated temperature profiles showed rather less variation. On the other hand, the number was larger (e.g., the number of layer and perceptrons were 5 and 30), the estimated temperature showed more complex curves. In addition, several outliers were found in the larger number of layers and perceptrons.

4. RESULTS OF NEURAL KRIGING APPROACH

4.1 Variogram of temperature data

Variogram of temperature data at boreholes was calculated to reveal spatial structure statistically. To satisfy second-order stationary, a best-fit logarithm function of temperature profile in depth was obtained in a least-square sense. Then, the logarithm function was subtracted from observed temperature data [Masaji, 2005]. Using the data after the subtraction, we estimated one-dimensional variogram. As a theoretical variogram model, exponential model was used. The estimated variogram and a best-fit theoretical model are plotted in Figure 8. Because of the fitness between experimental and theoretical variogram, it can be said that the best-fit exponential model properly represents the underlying statistical structure.

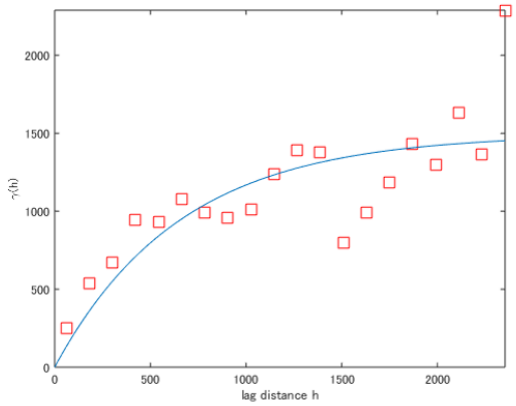

Figure 8: Variogram of temperature data after removal of a best-fit logarithm function. Red squares indicate variogram of observed data, and a blue line indicates a best-fit theoretical model.

4.2 The estimation of temperature at well WD1

The neural kriging estimation was performed according to section 2.2. As used in section 3, the teaching data is all temperature data except WD1, and the validation data is temperature data at WD1. The numbers of layers and perceptrons per a layer were set to be 3 and 20, respectively. Then, the errors of data and variogram were compared with neural network and neural kriging temperature estimation based on resistivity data. The error of variogram is defined as follows:

$$Er_v = \sqrt{\frac{\sum_i \left(\gamma(h_i) - \gamma_e(h_i)\right)^2}{\sum_i \gamma_e(h_i)^2}} \qquad (7)$$

By using neural network approarch, the error of data was 19.9 % and the error of variogram was 19.3 %. On the other hand, the errors of data and variogram were 15.6 % and 7.5 % in the case of neural kriging approach. Since variogram were considered to construct a neural network, the statistical structure was reproduced more accurately in neural kriging approach compared with neural network approach. Notably, the error of data also reduced by applying neural kriging approach.

Table 2: Comparison of the error of data and variogram by means of approaches based on neural network and neural kriging.

	The error of data [%]	The error of variogram [%]
Based on Neural Network	19.9	19.3
Based on Neural Kriging	15.6	7.5

5. CONCLUSION

In this study, we examined the characteristics of neural network approach with resistivity to estimate temperature at a deeper location. We showed the importance of teaching data selection, as the estimation of temperature at a well located far from teaching data was less accurate. We also showed that the number of layers and perceptrons was one of important parameters. The error of the deepest well (WD1) was optimal when the number of layers was 4 and the number of perceptrons per a layer was 15. In addition, we proposed an approach using neural kriging based on resistivity. Since neural kriging account for both the error of data and variogram, the estimated temperature structure can have optimal structure statistically. In fact, the errors of data and variogram reduced by applying the neural kriging-based approach. One of the limitation of these methods is that the physical mechanisms of temperature propagation have not been considered. This would be a future improvement. This study provides the characteristics and the effectiveness of subsurface temperature estimation by neural network and neural kriging approach with resistivity data.

ACKNOWLEDGEMENTS

Authors acknowledge Tohoku Sustainable & Renewable Energy Co. Inc. for providing temperature data.

REFERENCES

Calderon-Macias, C., Sen, M.K. and Stoffa, P.L.: Artificial neural networks for parameter estimation in geophysics. *Geophysical Prospecting*, Vol.48, pp. 21 – 47 (2000).

Hanano, M.: Hydrothermal convection system of the Kakkonda geothermal field, Japan. *Proc. World Geothermal Congress 1995*, Vol.3, pp. 1629 – 1634 (1995).

Ikeuchi, K.: High-temperature measurement in well WD-1A and the thermal structure of the Kakkonda geothermal system, Japan. *Geothermics*, Vol.27, pp. 591 – 607 (1998).

Kasai, K.: The origion of hypersaline liquid in the quaternary Kakkonda granite, sampled from well WD-1a, Kakkoda geothermal system, Japan. *Geothermics*, Vol.27, pp. 631 – 645 (1998).

Kato, O.: Fracture systematics in and around well WD-1 Kakkonda geothermal field, Japan. *Geothermics*, Vol.27, pp. 609 – 629 (1998).

Koike, K., Matsuda, S. and Gu, B.: Evaluation of the interpolation accuracy of neural kriging with application to temperature distribution analysis. *Mathematical Geology*, Vol.3, pp. 421 - 448 (2001).

Masaji T.: Geostatistical analysis of geothermal temperatures in Yanaidzu-Nishiyama geothermal field northeastern Japan. *J. Geotherm. Res. Soc. Japan*, Vol.27, pp. 233 – 247 (2005).

Rumelhart D. and McClelland J.: Parallel Distributed Processing. *MIT Press, Cambridge USA*, pp. 576 (1988).

Spichak, V.V. and Zakharova, O.K.: The application of an indirect electromagnetic geothermometer to temperature extrapolation in depth. *Geothermal Prospecting*, Vol. 57, pp. 653 – 644 (2009).

Spichak, V.V., Zakharova, O.K. and Rybin A.K.: Estimation of near-surface temperature by means of magnetotelluric sounding. *Proc. XXXII Workshop on Geothermal Reservoir Engineering*, Standford. (2007).

Sen, M.K. and Stoff P.L.: Global optimization method in geophysical inversion. Elsevier Science B. V., Amsterdam. (1995).

Tian, B., Wang, L., Kashiwaya, K. and Koike, K.: combination of well-logging temperature and thermal remote sensing for characterization of geothermal resources in Hokkaido, northern Japan. *Remote Sens.*, Vol. 7, pp. 2647 – 2667 (2015).

Uchida, T., Lee, T.J. and Cerv, V.: 3-D inversion of magnetotelluric data in the Kakkonda geothermal field, northern Japan. *Proc. 6th SEGJ international symposium*, Japan. (2003).

van der Baan, M. and Jutten, C.: Neural networks in geophysical application. *Geophysics*, Vol.65, pp. 1032 – 1047 (2000).

Yokoyama, H., Nakatsuka, K., Abe, M. and Watanabe, K.: Temperature dependency of electrical resistivity of water saturated and the possibility of underground temperature estimation. *Journal of the Geothermal Research Society of Japan*, Vol.5, pp. 103 – 120 (1983).